MSSM precision physics at the Z resonance

S. Heinemeyer[1], W. Hollik[2], <u>A.M. Weber</u>[2] [a], and G. Weiglein[3]

[1] Instituto de Fisica de Cantabria (CSIC-UC), Santander, Spain
[2] Max-Planck-Institut für Physik (Werner-Heisenberg-Institut), Föhringer Ring 6, D–80805 Munich, Germany
[3] IPPP, University of Durham, Durham DH1 3LE, U.K.

Abstract. LEP and SLC provide accurate data on the process $e^+e^- \to f\bar{f}$ at the Z resonance. The GigaZ option at a future linear e^+e^- collider (ILC) will further improve these measurements. As a consequence, theory predictions with sufficiently smaller errors are necessary in order to fully exploit the experimental accuracies and to derive indirect bounds on the scales of new physics. Here we review the currently most accurate predictions of the Z pole observables (e.g. $\sin^2\theta_{\mathrm{eff}}$, Γ_Z, σ^0_{had}) in the context of the Minimal Supersymmetric Standard Model (MSSM). These predictions contain the complete one-loop results including the full complex phase dependence, all available MSSM two-loop corrections, as well as all relevant Standard Model contributions.

PACS. 12.60.Jv Supersymmetric models – 12.15.Lk Electroweak radiative corrections

1 Introduction

Z boson physics is well established as a cornerstone of the Standard Model (SM) [1]. Many (pseudo-) observables [2] have been measured with high accuracy at LEP and SLC using the processes (mediated at lowest order by photon and Z boson exchange)

$$e^+e^- \to f\bar{f}, \qquad f \neq e, \tag{1}$$

at a center of mass energy $\sqrt{s} \approx M_Z$. In particular these are the effective leptonic weak mixing angle at the Z boson resonance, $\sin^2\theta_{\mathrm{eff}}$, Z boson decay widths to SM fermions, $\Gamma(Z \to f\bar{f})$, the invisible width, Γ_{inv}, the total width, Γ_Z, forward-backward and left-right asymmetries, A_{FB} and A_{LR}, and the total hadronic cross section, σ^0_{had}. Here we focus on $\sin^2\theta_{\mathrm{eff}}$ and Γ_Z, as these two observables show the strongest sensitivity on effects due to virtual SUSY particles [3].

Together with the measurement of the mass of the W boson, M_W, and the mass of the top quark, m_t, the Z pole observables have been instrumental in bounding the mass of the SM Higgs boson, the last free parameter of the model. In a combined fit containing Z pole observables, W mass and W decay width, the indirect constraints predict a SM Higgs boson mass of $M_H = 76^{+33}_{-24}$ GeV, with an upper limit of $M_H \leq 144$ GeV at the 95% C.L. [1].

In order to fully exploit the high-precision measurements, the theoretical uncertainty in the predictions of the (pseudo-) observables should be sufficiently smaller than the experimental errors (in view of the anticipated ILC precisions [4,5] for the Z observables this is

a particularly challenging task). As a step in this direction we compute the currently most precise predictions for the observables at the Z resonance [3]. These contain the full one-loop result, all available higher order MSSM terms and all relevant SM contributions. For the first time we include the full phase dependence at the one-loop level.

2 The Z pole observables

Z pole pseudo observables are commonly defined and calculated in an effective coupling approach. This approach exploits the fact that the dominant contributions to the process $e^+e^- \to f\bar{f}$ at $s \sim M_Z^2$ stem from resonant Z boson exchange diagrams. Non-resonant terms arise from photon exchange diagrams and box contributions, both of which are accounted for as part of the unfolding procedure from the experimental data (see Refs. [2,3] for details). The electroweak radiative corrections can thus be absorbed into effective vector couplings, g_V^f, and axial vector couplings, g_A^f. These effective couplings are in turn used to define effective fermionic mixing angles (at Born level these coincide with the weak mixing angle, $\sin\theta_{\mathrm{w}} \equiv s_{\mathrm{w}}$)

$$\sin^2\theta_{\mathrm{eff}}^f := \frac{1}{4|Q^f|}\left(1 - \mathrm{Re}\left[\frac{g_V^f}{g_A^f}\right]\right) = s_{\mathrm{w}}^2 \mathrm{Re}\left[\kappa_f\right] \tag{2}$$

and partial decay widths

$$\Gamma_f = N_c^f \frac{\alpha}{3} M_Z \left(\left|g_V^f\right|^2 R_V^f + \left|g_A^f\right|^2 R_A^f\right). \tag{3}$$

The latter are commonly expressed as [2]

$$\Gamma_f = N_c^f \bar{\Gamma}_0 \left|\rho_f\right| \left(4(I_3^f - 2Q^f s_{\mathrm{w}}^2 \left|\kappa_f\right|)^2 R_V^f + R_A^f \right), \tag{4}$$

with

$$\bar{\Gamma}_0 = \frac{G_\mu M_Z^3}{24\sqrt{2}\pi} \tag{5}$$

and ρ_f derived from the axial vector couplings as detailed in Ref. [3]. In the above equations, Q^f, I_3^f and N_c^f stand for the charge, third isospin component and colour factor of the respective fermion f. The radiation factors $R_{V,A}^f$ account for QED and QCD interaction of the final state fermions in the decay $Z \to f\bar{f}$. Tau lepton and more importantly bottom quark mass effects also enter via $R_{V,A}^f$. The effective mixing angles defined in eq. (2) are intimately realted to the forward backward and left right asymmetries measured at LEP and SLC. The total Z boson width is obtained by summing over all partial widths Γ_f

$$\Gamma_Z = \sum_{f=\nu,l,q} \Gamma_f . \tag{6}$$

3 One-loop result and higher order terms

The computation of our MSSM predictions for the observables at the Z resonance consists of two main steps: the computation of the full MSSM one-loop results, for the first time under consideration of $\mathcal{CP}$-violating complex MSSM parameters, and the inclusion of all available higher order contributions from SM and MSSM. Details of the calculations, which are briefly summarised in the following, can again be found in Ref. [3].

To accomplish our first goal we renormalise the $Zf\bar{f}$ vertex in the relevant parameters and compute all contributing MSSM one-loop graphs and counterterms. All relevant Feynman graphs are calculated making use of the packages `FeynArts` [7] and `FormCalc` [8]. As regularisation scheme dimensional reduction [9] is used, which allows a mathematically consistent treatment of UV-divergences in supersymmetric theories at the one-loop level. The inclusion of loop corrected Higgs masses and couplings in the complex MSSM is another new feature of our calculation. Our implementation is performed in accordance with the program `FeynHiggs` [10,11] and the discussion in Ref. [12]. We furthermore resum the $\tan\beta$ enhanced bottom Yukawa couplings following an effective coupling approach [13]. For the first time we perform a full one-loop calculation for decay of the Z boson into neutralino pairs, $Z \to \tilde{\chi}_1^0 \tilde{\chi}_1^0$, which contributes to the invisible width and consequently also the total width of the Z boson, provided $m_{\tilde{\chi}_1^0} < M_Z/2$.

In Ref. [3] we give an exact description of the higher order terms which are included in our predictions for the observables at the Z resonance. Our philosophy regarding the inclusion of higher order terms is strongly influenced by fact that the theoretical evaluation of

the Z pole observables in the SM is significantly more advanced than in the MSSM (see Ref. [14] for a recent discussion of the state-of-the-art results in the SM). In order to obtain the most accurate predictions within the MSSM it is therefore desireable to take all known SM corrections into account. This can be done by writing the MSSM prediction for a quantity $x = g_{V,A}^f, \rho_f, \kappa_f, \ldots$ as

$$x^{\mathrm{MSSM}} = x^{\mathrm{SM}}\big|_{M_H^{\mathrm{SM}}=M_{h_1}} + \underbrace{x^{\mathrm{MSSM-SM}}}_{\equiv x^{\mathrm{SUSY}}}, \tag{7}$$

where x^{SM} is the prediction in the SM with the SM Higgs boson mass set to the lightest MSSM Higgs boson mass, M_{H_1}, and $x^{\mathrm{MSSM-SM}} \equiv x^{\mathrm{SUSY}}$ denotes the difference between the MSSM and the SM prediction. In order to obtain x^{MSSM} according to eq. (7) we evaluate $x^{\mathrm{MSSM-SM}}$ at the level of precision of the known MSSM corrections, while for x^{SM} we use the currently most advanced result in the SM including all known higher-order corrections. As a consequence, x^{SM} takes into account higher-order contributions which are only known for SM particles in the loop, but not for their superpartners (e.g. two-loop electroweak corrections to $\Delta\kappa$ beyond the leading Yukawa contributions). Besides including all known higher order SM contributions, we also account for all available generic SUSY two-loop terms [15,16], which enter as universal corrections via the ρ parameter.

4 Dependence on complex parameters

As already mentioned, $\sin^2\theta_{\mathrm{eff}}$ and Γ_Z are the two Z observables which show the strongest sensitivity on effects of new physics. We therefore focus on these two observables in the following. Analyses including $\sigma_{\mathrm{had}}^0, R_l, R_b$ etc. can be found in Refs. [3,6]. Detailed numerical studies showed [3] that the dependence on the sfermion mass parameters is much stronger than on the chargino/higgsino parameters. We therefore only investigate the dependence on the phases of A_t and A_b. As for $\Delta r/M_W$ [17], we find that the effective couplings $g_{V,A}^{f,(\alpha)}$ only depend on the absolute values $|X_t|$, $|X_b|$ of the off-diagonal entries in the $\tilde{t}$ and $\tilde{b}$ mass matrices, where $X_t = A_t - \mu/\tan\beta$, $X_b = A_b - \mu\tan\beta$. Thus, the phases of μ, A_t and A_b only enter in the combinations $(\phi_{A_{t,b}} + \phi_\mu)$, giving rise to modifications of the squark masses and mixing angles. It furthermore follows that the impact of ϕ_{A_t} (ϕ_{A_b}) on the sfermion masses is stronger for low (high) $\tan\beta$.

In Figs. 1 we show $\sin^2\theta_{\mathrm{eff}}$ and Γ_Z as a function of ϕ_{A_t} (with $\phi_\mu = \phi_{A_b} = 0$), for different values of $\tan\beta$ (varied from $\tan\beta = 5$ to $\tan\beta = 45$). Shown in the green-shaded bands are the current experimental values in their 1σ range. Using the same conventions as in Refs. [3,17], the other parameters are set to $M_{\tilde{f}} = M_{H^\pm} = M_2 = m_{\tilde{g}} = 500$ GeV, $|A_{t,b,\tau}| = |\mu| = 1000$ GeV, $\phi_{M_1} = \phi_{M_2} = \phi_{\tilde{g}} = 0$.

As expected, the dependence of $\sin^2\theta_{\mathrm{eff}}$ and Γ_Z on ϕ_{A_t} is most pronounced for small $\tan\beta$. The variation of ϕ_{A_t} in this case gives rise to a shift in the

two precision observables by 1–2σ. The effect becomes smaller for increasing $\tan\beta$, up to $\tan\beta = 15$. On the other hand, for high $\tan\beta$ the lighter $\tilde{b}$ mass becomes rather small for the parameters chosen in Figs. 1, reaching values as low as about 100 GeV for $\tan\beta = 45$. This leads to a sizable shift of ~ 1–2σ in the Z observables already for vanishing phases. The slight rise in the dependence on ϕ_{A_t} for $\tan\beta \geq 25$ is due to the overall enlarged SUSY contributions which occur for large $\tan\beta$ and the resulting low sbottom masses. We checked that the dependence on ϕ_{A_t} is in general significantly larger than the dependence on ϕ_{A_b}.
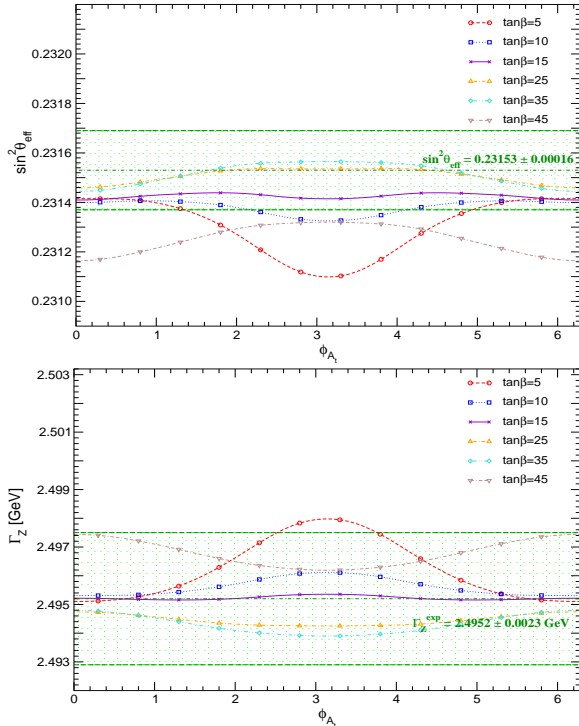
	Parameter	Range
sleptons	M_{L_i}, M_{E_i}	100 to 2000 GeV
squarks	$M_{Q_i}, M_{U_i}, M_{D_i}$	100 to 2000 GeV
	A_t, A_b	-2000 to 2000 GeV
gauginos	M_1, M_2	100 to 2000 GeV
	M_3	195 to 1500 GeV
Higgs	M_A	90 to 1000 GeV
	$\tan\beta$	1.1 to 60
	μ	-2000 to 2000 GeV

Table 1. MSSM parameter ranges in the unconstrained random parameter scan shown in Figs. 2 and 3. Family indices i run from 1 to 3, where the respective parameters are varied independently. All phases are set to zero.

Fig. 2. The predictions within the two models give rise to two bands in the m_t–$\sin^2\theta_{\text{eff}}$ plane with only a relatively small overlap region (indicated by a dark-shaded (blue) area). The allowed parameter region in the SM (the medium-shaded (red) and dark-shaded (blue) bands) arises from varying the only free parameter of the model, the mass of the SM Higgs boson, from $M_H^{\text{SM}} = 114$ GeV, the LEP exclusion bound [20] (lower edge of the dark-shaded (blue) area), to 400 GeV (upper edge of the medium-shaded (red) area). The very light-shaded (green), the light shaded (green) and the dark-shaded (blue) areas indicate allowed regions for the unconstrained MSSM. In the very light-shaded region at least one of the ratios $m_{\tilde{t}_2}/m_{\tilde{t}_1}$ or $m_{\tilde{b}_2}/m_{\tilde{b}_1}$ exceeds 2.5 (we work in the convention that $m_{\tilde{f}_1} \leq m_{\tilde{f}_1}$), while the decoupling limit with SUSY masses of $\mathcal{O}(2)$ TeV yields the upper edge of the dark-shaded (blue) area. Thus, the overlap region between the predictions of the two models corresponds in the SM to the region where the Higgs boson is light, i.e., in the MSSM allowed region ($M_h \lesssim 130$ GeV [10,11]). In the MSSM it corresponds to the case where all superpartners are heavy, i.e., the decoupling region of the MSSM. The 68% C.L. experimental results for $m_t = (170.9 \pm 1.8)$ GeV [21] and $\sin^2\theta_{\text{eff}}$ are indicated in the plot. As can be seen from Fig. 2, the current experimental 68% C.L. region for m_t and $\sin^2\theta_{\text{eff}}$ is in good agreement with both models and does not indicate a preference for either of the two. The prospective accuracies for the Tevatron/LHC ($\delta\sin^2\theta_{\text{eff}}^{\text{Tevatron/LHC}} = 0.00016$, $\delta m_t^{\text{Tevatron/LHC}} = 1$ GeV)) and the future ILC with GigaZ option ($\delta\sin^2\theta_{\text{eff}}^{\text{ILC/GigaZ}} = 0.000013$, $\delta m_t^{\text{ILC/GigaZ}} = 0.1$ GeV) are also shown in the plot (using the current central values), indicating the strong potential for a significant improvement of the sensitivity of the electroweak precision tests [5] (see Ref. [22] for a recent review of the anticipated errors at future colliders).

Fig. 1. Prediction for $\sin^2\theta_{\text{eff}}$ and Γ_Z as function of the phase of the trilinear coupling A_t. The other SUSY parameters are: $M_{\tilde{f}} = M_{H^\pm} = M_2 = m_{\tilde{g}} = 500$GeV, $A_\tau = A_t = A_b = \mu = 1000$ GeV, $\phi_\mu = \phi_{M_1} = \phi_{M_2} = \phi_{\tilde{g}} = 0$, $\phi_{A_b} = 0$

5 MSSM parameter scans

We now investigate the behaviour of $\sin^2\theta_{\text{eff}}$, the Z observable most sensitive to higher order corrections, by scanning over a broad range of the SUSY parameter space. The SUSY parameters given in Tab. 1 are varied independently of each other, within the given range, in a random parameter scan. Unlike Refs. [6,18,19], where our results for the electroweak precision observables were already employed in CMSSM multiparameter analyses, the scans in this section are entirely unconstrained, apart from the fact that we require the Higgs mass bounds and direct SUSY particle exclusions limits from LEP searches to hold.

The SM and the MSSM predictions for $\sin^2\theta_{\text{eff}}$ as a function of m_t, obtained from the scatter data with m_t as an additional free parameter, are compared in

In Fig. 3 we show the combination of M_W [17] and $\sin^2\theta_{\text{eff}}$ with the top quark mass varied in the range of 165 GeV to 175 GeV. The ranges of the other varied parameters and the colour coding are the same as in Fig. 2. The current 68% C.L. experimental results for M_W and $\sin^2\theta_{\text{eff}}$ are indicated in the plot. The region of the SM prediction inside todays 68% C.L. ellipse corresponds to relatively large m_t values, outside the

current experimental range of $m_t = (170.9 \pm 1.8)$ GeV. Thus, the combination of M_W and $\sin^2 \theta_{\text{eff}}$ exhibits a slight preference for the MSSM over the SM. The anticipated future improvements in the measurements of M_W and $\sin^2 \theta_{\text{eff}}$ are again indicated.
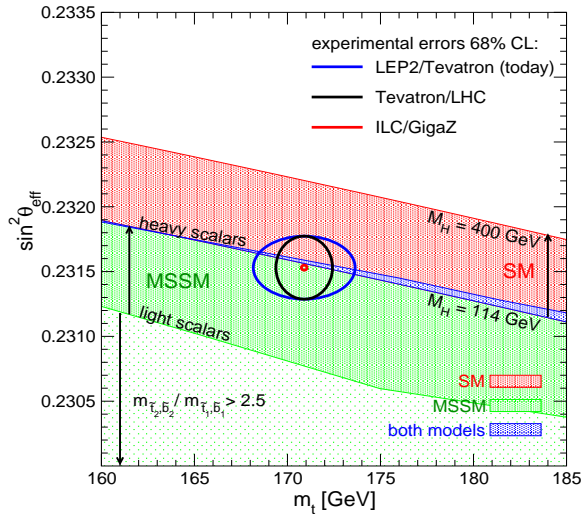

Fig. 2. Unconstrained MSSM random parameter scan for $\sin^2 \theta_{\text{eff}}$ as a function of m_t over the ranges given in Tab. 1. Todays 68% C.L. level ellipses as well as future precisions, drawn around todays central value, are indicated in the plot.
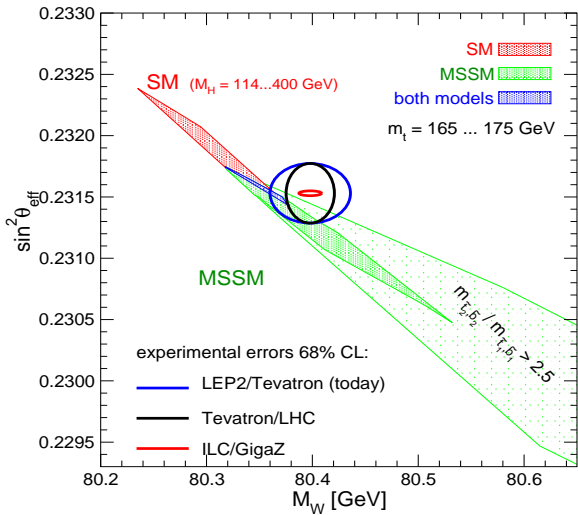

Fig. 3. Unconstrained MSSM random parameter scan over the ranges given in Tab. 1 and $m_t = 165 \ldots 175$ GeV. Shown is the combination of M_W and $\sin^2 \theta_{\text{eff}}$. Todays 68% C.L. level ellipses as well as future precisions, drawn around todays central value, are indicated in the plot.

References

1. [The ALEPH, DELPHI, L3, OPAL, SLD Collaborations, the LEP Electroweak Working Group, the SLD Electroweak and Heavy Flavour Groups], Phys. Rept.

427 (2006) 257, hep-ex/0509008; [The ALEPH, DELPHI, L3 and OPAL Collaborations, the LEP Electroweak Working Group]; M. W. Grunewald, talk given at the *EPS HEP 2007 conference Manchester, England, July, 2007*, arXiv:0709.3744 [hep-ph]; see also: `lepewwg.web.cern.ch/LEPEWWG/Welcome.html`.

2. D. Bardin et al., in *Precision Calculations for the Z Resonance*, Yellow report CERN 95-03, eds. D. Bardin, W. Hollik and G. Passarino; D. Bardin, M. Grünewald and G. Passarino, hep-ph/9902452.

3. S. Heinemeyer, W. Hollik, A.M. Weber, and G. Weiglein, arXiv:0710.2972 [hep-ph].

4. R. Hawkings and K. Mönig, *EPJdirect* **C 8** (1999) 1.

5. S. Heinemeyer, T. Mannel and G. Weiglein, hep-ph/9909538; J. Erler, S. Heinemeyer, W. Hollik, G. Weiglein and P. Zerwas, *Phys. Lett.* **B 486** (2000) 125; J. Erler and S. Heinemeyer, hep-ph/0102083.

6. O. Buchmueller et al., arXiv:0707.3447 [hep-ph].

7. J. Küblbeck, M. Böhm and A. Denner, *Comput. Phys. Commun.* **60** (1990) 165; T. Hahn, *Nucl. Phys. Proc. Suppl.* **89** (2000) 231; *Comput. Phys. Commun.* **140** (2001) 418 ;T. Hahn and C. Schappacher, *Comput. Phys. Commun.* **143** (2002) 54; The program is available via `www.feynarts.de`.

8. T. Hahn and M. Pérez-Victoria, *Comput. Phys. Commun.* **118** (1999) 153; see: `www.feynarts.de/formcalc` .

9. W. Siegel, *Phys. Lett.* **B 84** (1979) 193; D. Capper, D. Jones and P. van Nieuwenhuizen, *Nucl. Phys.* **B 167** (1980) 479; W. Siegel, *Phys. Lett.* **B 94** (1980) 37; L. Avdeev, *Phys. Lett.* **B 117** (1982) 317; L. Avdeev and A. Vladimirov, *Nucl. Phys.* **B 219** (1983) 262; I. Jack and D. Jones, in *Perspectives on Supersymmetry*, ed. G. Kane (World Scientific, Singapore), p. 149; D. Stöckinger, *JHEP* **0503** (2005) 076.

10. S. Heinemeyer, W. Hollik and G. Weiglein, *Comput. Phys. Commun.* **124** 2000 76; *Eur. Phys. J.* **C 9** (1999) 343; The code is accessible via `www.feynhiggs.de` .

11. G. Degrassi, S. Heinemeyer, W. Hollik, P. Slavich and G. Weiglein, *Eur. Phys. J.* **C 28** (2003) 133.

12. M. Frank, T. Hahn, S. Heinemeyer, W. Hollik, H. Rzehak, and G. Weiglein, *JHEP* **02** (2007) 047.

13. M. Carena, D. Garcia, U. Nierste and C. Wagner, *Nucl. Phys.* **B 577** (2000) 577.

14. M. Awramik, M. Czakon and A. Freitas, *JHEP* **11** (2006) 048.

15. A. Djouadi, P. Gambino, S. Heinemeyer, W. Hollik, C. Jünger and G. Weiglein, *Phys. Rev. Lett.* **78** (1997) 3626. *Phys. Rev.* **D 57** (1998) 4179, hep-ph/9710438.

16. J. Haestier, S. Heinemeyer, D. Stöckinger and G. Weiglein, *JHEP* **0512** (2005) 027.

17. S. Heinemeyer, W. Hollik, D. Stöckinger, A.M. Weber and G. Weiglein, *JHEP* **0608** (2006) 052.

18. B. Allanach, C. Lester, and A.M. Weber, *JHEP* **0612** (2006) 065; C. Allanach, K. Cranmer, C. Lester, and A.M. Weber, *JHEP* **0708** (2007) 023.

19. J. Ellis, S. Heinemeyer, K. Olive, A.M. Weber and G. Weiglein, *JHEP* **0708** (2007) 083.

20. G. Abbiendi et al. [ALEPH, DELPHI, L3, OPAL Collaborations and LEP Working Group for Higgs boson searches], *Phys. Lett.* **B 565** (2003) 61.

21. Tevatron Electroweak Working Group, hep-ex/0703034.

22. J. Erler, (2007), `hep-ph/0701261`.